Atmospheric Environment 199 (2019) 265–273

Contents lists available at ScienceDirect

Atmospheric Environment

journal homepage: www.elsevier.com/locate/atmosenv

Formation of oxidized organic compounds from Cl-initiated oxidation of toluene

Surya Venkatesh Dhulipala, Sahil Bhandari, Lea Hildebrandt Ruiz*

McKetta Department of Chemical Engineering, The University of Texas at Austin, Austin, TX, 78712, USA

ARTICLE INFO

Keywords:
Toluene
Chlorine
Oxidation
Secondary organic aerosol
Environmental chamber experiments

ABSTRACT

The formation of secondary organic aerosol (SOA) from toluene can impact urban air quality and therefore human health. Most SOA studies have focused on OH chemistry; however recent work suggests that chlorine atoms (Cl) may affect tropospheric chemistry more than previously assumed. This work focuses on SOA formation from Cl-initiated oxidation of toluene under different conditions. The fast reaction between Cl and toluene enabled complete consumption of toluene in environmental chamber experiments and aging of the toluene SOA. A high resolution time-of-flight chemical ionization mass spectrometer was used to observe several generations of gas-phase products. The presence of nitric oxides (NO_x) appears to delay the formation of later generation products. Data from an aerosol chemical speciation monitor suggest that all SOA formed had high oxidation state, and that the bulk organic composition was different for SOA from Cl-dominated reactions compared to SOA from OH-dominated reactions. Addition of oxidant after all toluene had been consumed did not result in a significant change in the organic aerosol oxidation state, suggesting that the system may have reached an oxidative end-point in the particle phase.

1. Introduction

Inhalation of fine particulate matter (PM) is associated with increased mortality (Brook et al., 2016; Cohen et al., 2017; Hamra et al., 2014; Kampa and Castanas, 2008; Peng et al., 2008). Volatile organic compounds (VOCs) undergo chemical reactions in the atmosphere, and reaction products can partition to the particle phase as secondary organic aerosol (SOA) (Pankow, 1994; Saxena and Hildemann, 1996), increasing concentrations of tropospheric PM. Atmospheric SOA also undergoes progressive oxidation or "aging", which can alter SOA concentrations and oxidation state (Hallquist et al., 2009; Heald et al., 2010; Jimenez et al., 2009; Kroll et al., 2009; Ng et al., 2010; Poschl, 2005; Robinson et al., 2007; Rudich et al., 2007; Shrivastava et al., 2008).

Toluene (methyl benzene) is a small aromatic compound and is an important component of solvents, paints (Fabri et al., 2000) and commercial gasoline fuels (Alramadan et al., 2016; Diehl and Di Sanzo, 2005). Urban toluene concentrations have been reported to vary from 1 to 200 ppb, (Fortner et al., 2009; Wang et al., 2009). The oxidation of toluene by the hydroxyl radical (OH) and formation of SOA have been studied extensively (Birdsall et al., 2010; Birdsall and Elrod, 2011; Calvert et al., 2002; Chhabra et al., 2011; Hildebrandt et al., 2009; Hildebrandt Ruiz et al., 2015; Molina et al., 1999; Ng et al., 2007; Noda et al., 2009; Suh et al., 2002, 2003; Zhang et al., 2012). OH is often the most abundant tropospheric free radical during the day with concentrations on the order of 10^6 molecules cm^{-3}(Mallik et al., 2018), and the reactions of toluene with the nitrate radical or ozone are slow. However, ambient measurements suggest that tropospheric concentrations of chlorine atoms (Cl) are higher than previously assumed (Chang and Allen, 2006; Faxon and Allen, 2013; Graedel and Keene, 1995; Tanaka et al., 2000), and that chlorine chemistry may be important in continental as well as coastal environments (Behnke et al., 1997; Finlayson-Pitts, 1993; Finlayson-Pitts et al., 1989; Tanaka et al., 2000). Average daytime Cl radical concentrations in the marine boundary layer were estimated to be 3×10^5 molecules cm^{-3} with peak concentrations of 8×10^6 molecules cm^{-3} (Chang et al., 2004). Cl_2 concentrations up to 3.7×10^9 molecules cm^{-3} have been detected in marine air at night, suggesting a Cl_2 emissions source of 8.1×10^9 molecules $cm^{-3}day^{-1}$ (Spicer et al., 1998).

The toluene-Cl reaction rate constant is 6.2×10^{-11} cm^3 molecule $^{-1}s^{-1}$ (Wang et al., 2005), ten times larger than the toluene-OH reaction rate constant of 5.63×10^{-12} cm^3 molecule $^{-1}s^{-1}$ (Calvert et al., 2002). This implies that even when tropospheric Cl concentrations are relatively low, the reaction of toluene with Cl can be competitive with or even exceed the reaction rates of OH with toluene. The OH-initiated oxidation of toluene proceeds via OH-addition to the aromatic ring

* Corresponding author.
E-mail addresses: svd@utexas.edu (S.V. Dhulipala), sahilb@utexas.edu (S. Bhandari), lhr@che.utexas.edu (L. Hildebrandt Ruiz).

https://doi.org/10.1016/j.atmosenv.2018.11.002
Received 23 April 2018; Received in revised form 1 November 2018; Accepted 4 November 2018
Available online 12 November 2018
1352-2310/

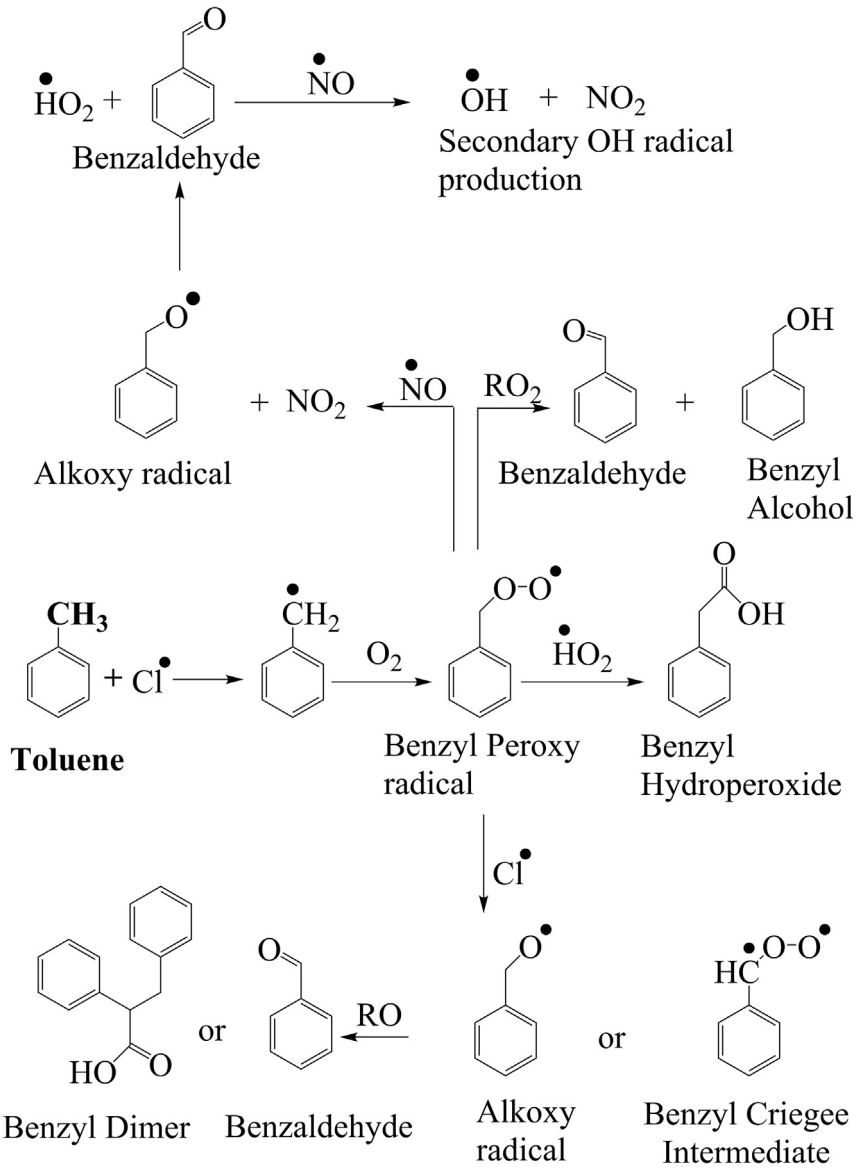

Fig. 1. Outline of reaction pathway for Cl-initiated oxidation of toluene, modified from several sources (Cai et al., 2008; Fantechi et al., 1998; Huang et al., 2014, 2012; Karlsson et al., 2001; Wang et al., 2005; Young et al., 2014).

(approximately 90%) or H-atom abstraction (Molina et al., 1999). The Cl-initiated oxidation of toluene proceeds primarily (if not exclusively) via H-atom abstraction to form benzyl peroxy radicals (Wang et al., 2005), which continue reacting to form major gas phase products including benzaldehyde, benzyl hydro peroxide and benzyl alcohol, benzyl methyl nitrate and peroxybenzoyl nitrate (Fantechi et al., 1998; Huang et al., 2014, 2012; Karlsson et al., 2001; Wang et al., 2005). In the absence of NO_x, peroxy radicals are expected to mostly undergo self-reaction leading to radical termination (Young et al., 2014). The presence of NO_x in the toluene + Cl system enhances radical propagation and formation of secondary radicals including OH. These OH radicals can further react with other intermediate products. Fig. 1 depicts first steps in the toluene-Cl reaction mechanism and Fig. S1 shows the continued oxidation of the benzyl Criegee intermediate.

This manuscript describes results from environmental chamber experiments focused on Cl-initiated oxidation of toluene leading to the formation of SOA. The fast reaction between toluene and Cl enabled complete precursor consumption and evaluation of SOA aging using different oxidants including OH and Cl radicals in the presence and absence of NO_x. Several generations of gas-phase products are observed and their qualitative trends evaluated. SOA yields are quantified and bulk SOA composition is evaluated.

2. Methods

2.1. Environmental chamber experiments

Experiments were conducted in the Atmospheric Physicochemical Processes Laboratory Experiments (APPLE) chamber at the University of Texas at Austin. The APPLE chamber is a 12 m^3 Teflon® bag (Welch Fluorocarbon) suspended in a temperature controlled room lined with UVA lamps (204 GE T12 Blacklights; peak emission at 368 nm). The NO_2 photolysis rate was determined to be 0.30 min^{-1} when all UV lights are used and 0.13 min^{-1} when 40% of UV lights are used. Using a Cl_2 photolysis rate (j_{Cl2}) of 1×10^{-3} s^{-1} at 40% UV lights (Faxon et al., 2018) and an initial Cl_2 concentration of 40 ppb, the estimated initial Cl production rate in this work is 290 ppb h^{-1}. In experiments with Cl as initiating radical (Expts. 1–7), 40% of UV lights were used to decrease Cl concentrations and slow the reaction.100% of UV lights were used in experiment with OH-initiated chemistry.

Ammonium sulfate (Sigma Aldrich, 99%) seed particles were created from a 0.01 M solution using an aerosol generation system (Brechtel Manufacturing, Inc. Model 9200). Molecular chlorine (Cl_2) was introduced into the chamber using a high-pressure gas cylinder from Airgas (106 ppm in N_2). In selected experiments, NO and NO_2 were added to the chamber using high-pressure gas cylinders from Airgas (48.73 ppm NO and 9.86 ppm NO_2 respectively). In some experiments, HONO was added as a source of OH and NO_x; HONO was prepared immediately before injection in a custom-made glass flask by adding a 0.05 M solution of sulfuric acid to a 0.1 M solution of sodium nitrite. The titrated HONO was then introduced into the chamber by flushing the flask with clean air at a flow rate of 2 lpm. H_2O_2 (Sigma Aldrich, 30% (w/w)) was added in some experiments as a source of OH radicals. It was introduced into the chamber by flushing clean air through a glass bottle containing the H_2O_2 solution at a flow rate of 2 lpm. Introducing H_2O_2 increased the relative humidity in the chamber by less than 2% - all experiments were conducted under dry conditions (< 5% RH). Similarly, microliters of toluene (Sigma Aldrich, 99%) were introduced into the chamber via the glass sampling tube. After the particles and gases were injected into the chamber and allowed to mix, the UV lights were switched on, photolyzing the oxidant precursors (e.g. HONO to OH + NO, Cl_2 to 2Cl or H_2O_2 to 2OH) and starting the oxidation reactions. Initial conditions and results of all experiments are summarized in Table 1. Instrument availability is summarized in Table S1.

The chamber was cleaned before each experiment by flushing it with dry clean air generated by a clean air generator (AADCO 737–11) at a flowrate exceeding 100 L per minute (LPM) for at least 12 h. Between experiments, "blank experiments" were conducted in which inorganic seed particles and Cl_2 were injected into the chamber at high concentrations and 100% of UV lights were turned on to remove residual organics which could be released from the Teflon® chamber surface.

2.2. Instrumentation

A high-resolution time-of-flight chemical ionization mass spectrometer (CIMS, Aerodyne Research Inc.) was used to measure gas-phase organic compounds. Detailed theory and operation of the CIMS are discussed elsewhere (Aljawhary et al., 2013; Bertram et al., 2011; Lee et al., 2014; Yatavelli et al., 2012). The instrument can be operated using different reagent ions; in this work hydronium-water clusters ($(H_2O)_n(H_3O)^+$) were used as chemical reagents and were generated by passing humidified ultra-high purity (UHP) N_2 through a ^{210}Po radioactive cartridge (NRD, P-2021) at 2 LPM into the ion-molecule reaction (IMR) chamber operating at 200 mbar pressure. An aerosol chemical speciation monitor (ACSM, Aerodyne Research Inc.) was used to determine the bulk chemical composition of submicron, non-refractory aerosol species in most experiments (Ng et al., 2011). In the ACSM, particles are flash-vaporized at 600 °C, the resulting vapors are ionized via electron impact ionization (EI), and the ions are measured by a quadrupole mass spectrometer (Ng et al., 2011). Calibration of the ACSM was performed with 300 nm size-selected ammonium nitrate and ammonium sulfate aerosol (generated from 0.005 M aqueous solutions) to determine the response factor for particulate nitrate and the relative ionization efficiencies (RIE) of ammonium and sulfate.

Particle volume and size distributions were measured using a scanning electrical mobility spectrometer (SEMS, Brechtel Model 2002) consisting of a differential mobility analyzer and a butanol condensation particle counter. The sheath and sample flow rates of the SEMS were set to 5 and 0.35 LPM, respectively, covering a 10–1000 nm size range. Concentrations of NO and O_3 were measured using Teledyne chemiluminescence NO_x and absorption O_3 monitors (200E and 400E, respectively). Concentrations of NO_2 were measured via a NO_2 monitor from Environnement (Model AS32M), which uses a cavity attenuated phase shift (CAPS) method to directly measure NO_2 (Kebabian et al., 2008). The advantage of this direct NO_2 measurement is that it does not rely on NO_2 conversion to NO and therefore does not suffer from interference by other oxidized nitrogen compounds including HONO, HNO_3 and organic nitrates (Winer et al., 1974).

2.3. Data analysis

Data from the CIMS were analyzed in IGOR Pro (WaveMetrics) using Tofware, the software provided with the instrument. The baseline was subtracted and the average peak shape was found so it could be used for high resolution analysis. After ions were identified in the high resolution spectrum, the peaks were integrated to yield a time series of ions. The CIMS sensitivity was corrected using the active chemical ionization mass spectroscopy (ACIMS) formula (de Gouw and Warneke, 2007), normalizing all product ion signals against the dominant reagent ion signals (H_3O^+, $H_5O_2^+$ and $H_7O_3^+$). For all experiments conducted, the sum of reagent signals was at least 10^3 times greater than the summed product signals. Initial toluene injected in each experiment was calculated based on a linear calibration of CIMS signal in the absence of UV lights. After UV lights were switched on, toluene could not be quantified reliably due to the presence of four nearby peaks at m/z 93 (Cubison and Jimenez, 2015): $C_6H_5O^+$, $C_3H_9O_3^+$, $C_7H_9^+$, and $C_4H_{13}O_2^+$ (Fig. S2). The CIMS was not calibrated for the product ions; thus, the analysis presented here focuses on qualitative trends, and the

Table 1
Experimental conditions and summary of results.

Exp	$[VOC]_0$ (ppb)	$[Cl_2/VOC]_0$ (ppb/ppb)	$[NO]_0$ (ppb)	f_{44}[d] (%)	f_{43}[d] (%)	C_{OA}[d] (μg m^{-3})	SOA Yield[d]	HCl^+/Org (%)[d]	% VOC reacted w/Cl[e]
1	51	0.78	< 2	17	3	70	0.36	5.1	100
2	54	2.1	< 2	16	3	136	0.67	6.5	100
3	37	2.2	19	18	3	113	0.82	7.3	91
4	39	1.04	21	18	5	32	0.22	4.5	84
5	53	1.5	< 2	17	4	100	0.50	5.0	100
6	43	0.94	< 2	19	3	53	0.33	6.9	100
7	22	2.0	18	25	3	15	0.17	10.1	88
8[a,b,c]	430	HOOH	< 2	16	9	10	N/A	0.60	0
9[a,b,c]	300	HONO	369	14	10	318	N/A	0.38	0
10[b,c]	490	0.08	490	15	10	294	N/A	0.66	21
11[b]	230	0.17	433	16	8	94	N/A	0.82	55

[a] No chlorine was added in these experiments.
[b] Toluene was not completely consumed in these experiments.
[c] 100% UV lights at beginning of experiment; all other experiments conducted at 40% UV lights.
[d] f_{44}, f_{43}, C_{OA} (μg m^{-3}), SOA yields and HCl^+/Org reported after 60 min of photo-oxidation. SOA yields were only calculated for experiments where modeling results suggested complete consumption of toluene.
[e] VOC reacted with Cl divided by total VOC reacted (with OH or Cl) based on modeling results.

gas-phase data are also normalized by the maximum signal of each ion for improved visualization.

Data from the ACSM were analyzed in Igor Pro using the software package ACSM Local, which includes a correction for relative ion transmission efficiency as well as changes in the flow rate throughout the experiment. The ACSM data were analyzed using the standard fragmentation table (Allan et al., 2004) to attribute ion fragments to four bulk species: organics, sulfate, ammonium and nitrate. The nitrate signal as measured by the ACSM (NO^+ and NO_2^+ fragments) was assumed to be due to organic nitrates because no free ammonium (which could form ammonium nitrate in high NO_x experiments) was introduced in these controlled experiments. Nitrate mass was hence added to organic mass for quantification of total organic aerosol formed. The relative ionization efficiency (RIE) of nitrate was used to calculate this (organic) nitrate mass. This is justified assuming that the organic nitrate molecules fragment before they are ionized, which is expected considering the thermal lability of organic nitrates and the flash vaporization at 600 °C utilized by the ACSM.

The UMR spectrum measured by the ACSM can be used to characterize the extent of oxidation of OA. The organic mass at m/z 44 mostly corresponds to the CO_2^+ ion and can be used as a proxy for highly oxidized organic aerosol; the organic mass at m/z 43 mostly corresponds to the $C_2H_3O^+$ ion and can be used as a proxy for moderately oxidized organic aerosol (Aiken et al., 2008, 2007; Canagaratna et al., 2015; Chhabra et al., 2011; Ng et al., 2010). It has become customary to characterize the extent of oxidation of the organic aerosol using the fraction of the total organic signal due to ions at m/z 44 and 43 (f_{44} and f_{43}). When plotting f_{44} versus f_{43}, ambient data fall within a triangular region (Ng et al., 2010); however, this is not necessarily the case for SOA formed in environmental chamber experiments (Chhabra et al., 2011).

The ACSM does not detect all sampled particles, primarily due to particle bounce at the vaporizer, resulting in a collection efficiency (CE) smaller than 1 (Ng et al., 2011). Collection efficiency and wall losses were accounted for by multiplying the ACSM concentrations of organics by the mass concentration ratio of initial sulfate (measured by the SEMS) and time-dependent sulfate measured by the ACSM (Hildebrandt et al., 2009). This correction accounts for depositional wall losses of particles and the condensation of organic vapors onto wall-deposited particles; it does not account for losses of organic vapors onto the clean Teflon® walls.

The organic aerosol yield is calculated as the ratio of the amount of OA formed divided by the mass of VOC precursor reacted (Table 1, Fig. S3). Due to the fast formation of organic aerosol and challenges with the quantification of toluene, OA yields were evaluated 1 h after start of photo-oxidation, only for Experiments 1–7 for which the model (see section 2.4) suggested > 97% of the toluene had been consumed after < 30 min. OA concentrations were stable after 30 min suggesting that OA formation had ceased and that most OA products were not photo labile. Due to the fast organic aerosol formation in these experiments, and since OA concentrations were evaluated after 60 min, the wall loss correction had only a small effect (< 5%) on organic aerosol concentrations and mass yields.

2.4. Box modeling and analysis

Box-modeling was conducted in the SAPRC framework (Carter et al., 2005; Carter and Heo, 2013) using the condensed carbon bond mechanism CB6 (Yarwood et al., 2010) with an updated gas-phase chlorine mechanism (Sarwar et al., 2012). Results from chamber characterization experiments were utilized to account for light intensity, leak rate and off-gassing of HONO and HCHO from chamber walls (see supplemental information for additional details). Initial measured reactant concentrations of toluene, nitrogen oxides (NO, NO_2), and chlorine gas (Cl_2) were used as inputs to the model. Two "dummy species" and corresponding reactions were added to the model to track the reaction of toluene with chlorine atoms (CLVTOL) and with OH (OHVTOL). HONO was not measured directly, but initial concentrations were estimated from the difference of NO_2 concentrations reported by the chemiluminescence NO_x monitor (where HONO is measured as NO_2) and CAPS NO_2 monitor (which does not detect HONO). The sensitivity of the chemiluminescent NO_x monitor to HONO has not been measured and was assumed to be equal to the sensitivity of NO. Initial HONO concentration in the model was varied within 10% to evaluate model sensitivity to this input, which was found to be low.

Experimental and modeled results for experiments 10 and 11 are shown in the SI (Figs. S3 and S4). Concentrations of NO_x and O_3 from the box model agree reasonably well with measurements. The box model's primary use was to estimate the extent of reaction of toluene with OH versus Cl (Table 1), and the chlorine chemistry in the box model is very limited. In experiments in which all toluene is consumed (Expts. 1–7), Cl concentrations in the model increase dramatically when all toluene has been consumed because no other hydrocarbon species are present in the model to react with Cl. In the actual experiment, Cl continues to react with toluene oxidation products – this is not represented in the model. Thus, in Table S2, we report model-predicted concentrations of OH and Cl 5 min after UV lights were turned on, when a significant fraction of toluene is present. Concentration of OH at this time range from 8×10^4–6×10^7 molecules cm^{-3}; concentrations of Cl range from 3×10^6–2×10^8 molecules cm^{-3}. The absolute OH and Cl radical concentrations are 1–2 orders of magnitude higher than typical ambient concentrations. The ratio of Cl and OH concentrations is similar to ambient conditions in those experiments which were aimed to achieve a balance of OH and Cl-initiated reactions (Expts. 10 and 11). Experiments conducted in this work thus allow evaluation of Cl-initiated chemistry as well as the interaction between Cl and OH-initiated chemistry, as expected to occur in the troposphere.

3. Results and discussion

All experiments formed SOA. The first few generations of gas-phase chemistry were observed with the CIMS, and the evolution of organic aerosol was observed with the ACSM. Fig. 2 (top panel) shows time series of gas and particle-phase species from Expt. 1, a typical low NO_x experiment (toluene + Cl) and time series from Expt. 4 (bottom panel), a typical high NO_x (toluene + Cl + NO_x) experiment. Gas-phase species shown in Fig. 2 are expected to form from toluene + Cl chemistry as shown in Fig. 1 and Fig. S1.

For experiments in which Cl was the dominant oxidant, nearly all toluene reacted away in less than 30 min of photo-oxidation (Fig. 2). This is quite different from experiments in which OH is the dominant oxidant, where less than half of the toluene reacts after several hours of photo-oxidation in this work and previous work (Hildebrandt et al., 2009; Hildebrandt Ruiz et al., 2015; Karlsson et al., 2001; Ng et al., 2007). The inability to react all or most of the toluene in the toluene + OH system poses challenges in investigating the aging of SOA formed from the oxidation of toluene (Hildebrandt et al., 2009; Hildebrandt Ruiz et al., 2015; Ng et al., 2007). Chlorine atoms thus enable studying toluene SOA aging, as explored in more detail in Section 3.2.

The SOA yields from Cl-initiated oxidation of toluene are in the range of SOA yields from OH-initiated oxidation of toluene reported by Hildebrandt et al. (2009) (Table 1; Fig. S5). The similar yields and the difference in reaction rate constants (~factor of 10) means that when Cl concentrations are a factor of 10 lower than OH concentrations, Cl and OH-initiated oxidation of toluene contribute similarly to the formation of toluene SOA.

3.1. Gas-phase products

Multi-generational products are formed within minutes of the start of photo-oxidation (Fig. 2). The CIMS provides the exact mass of ions

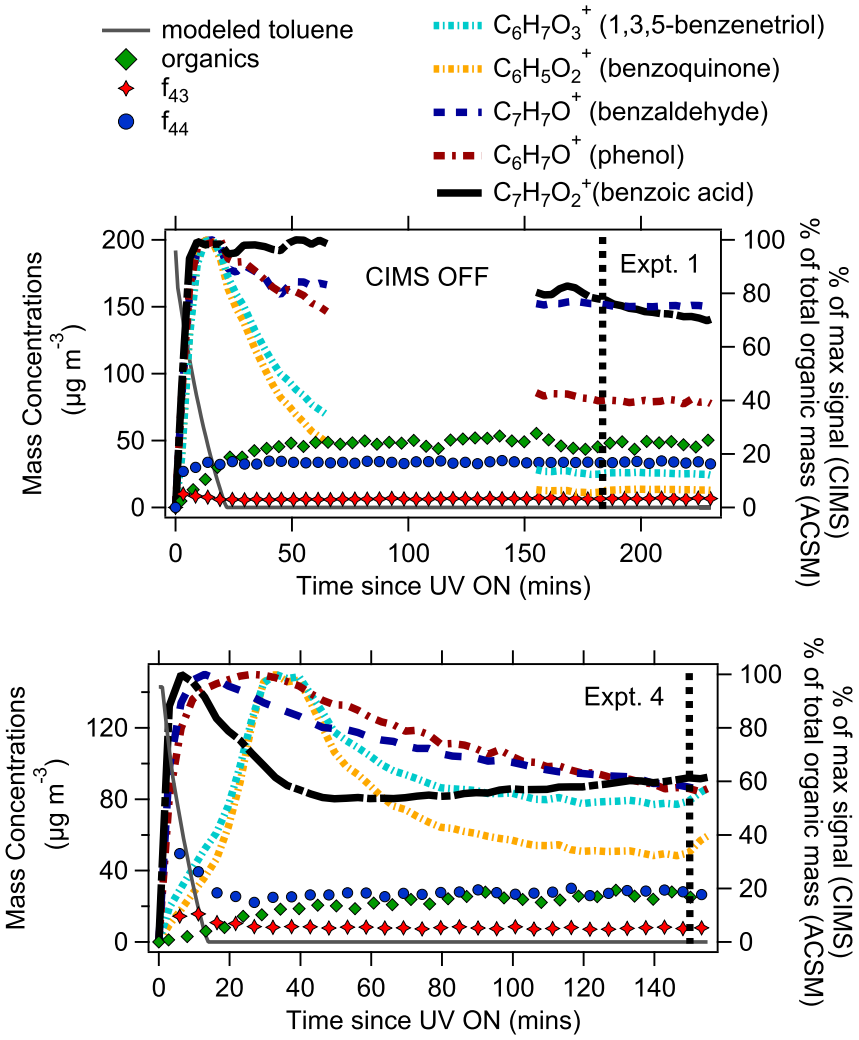

Fig. 2. Time series of wall-loss corrected OA concentration and modeled toluene decay (left vertical axis) and gas-phase products and f_{43}, f_{44} time series (right vertical axis) during experiment 1 (toluene + Cl; top panel) and experiment 4 (toluene + Cl + NO_x; bottom panel). The dotted black vertical line indicates the time when UV lights were switched off.

from which their molecular formulae can be derived; it does not provide information on molecular structure. The assignment to chemical species is based on molecular formulae and information about the reaction mechanism; however, some uncertainty remains. For example, the suggested product benzenetriol could be benzoquinone with an additional water molecule clustered to the ion – available measurements do not allow definite distinction between these two species. Considering the similarity in their qualitative trends, this does not affect the analysis presented below (which focuses on benzoquinone for simplicity). Higher-generation (more oxygenated) gas phase species were not observed in this work due to the choice of reagent ion - the water cluster CIMS is only sensitive to moderately oxygenated species.

While the presence of NO_x and OH affects the reaction pathway and can result in the formation of different reaction products, here we focus on products that are observed in all experiments. The formation of later generation products is consistently delayed in high NO_x experiments relative to low NO_x experiments (e.g. Fig. 2). This could be due to the presence of NO_x suppressing later-generation Cl chemistry and products; for example, benzoquinone is formed from continued Cl chemistry (Fig. S1). A further difference between high NO_x and low NO_x experiments specific to chlorine-initiated chemistry is the formation of $ClNO_2$ in the high NO_x environment, which can result in decreased concentrations of Cl atoms at the beginning of the experiment and a sustained source of Cl throughout the experiment. In contrast, in low NO_x experiments most of the Cl forms HCl, which is relatively stable to photolysis and does not result in significant recycling of Cl. While $ClNO_2$ was not measured in this work, box model results can provide some insights. For example, in Figs. S3 and S4 (Expts. 10 and 11), modeled $ClNO_2$ concentrations decrease after initial $ClNO_2$ formation but are constant when UV lights are turned off, suggesting $ClNO_2$ as a source of Cl. Another difference in the oxidative conditions between low and high NO_x experiments is the generation of secondary OH: in high NO_x experiments, a significant fraction of the toluene reacts with OH instead of with Cl (Table 1). The delay in formation of later generation products could thus be because the formation of $ClNO_2$ in the high NO_x experiments slows down the chemistry, the presence of NO_x initially inhibits the formation of the higher-generation products formed through the low NO_x pathway, and/or the presence of NO_x increases the importance of OH chemistry relative to Cl chemistry.

3.2. Organic aerosol bulk composition and oxidation state

Chlorine-initiated oxidation of toluene is thought to proceed primarily, if not exclusively, via hydrogen abstraction at the methyl group (Wang et al., 2005). However, later-generation chemistry could include chlorine-addition to double bonds, for example, those in benzoquinone. Thus, formation of organochlorides in later-generation chemistry is possible. Wang and Hildebrandt Ruiz (2017) evaluated the ability of the

ACSM to quantify organochlorides and pointed out that, under normal operating conditions and using standard ACSM analysis techniques, the ACSM generally under predicts concentrations of organochlorides. However, the ion signal at m/z 36 (HCl^+) seems to be a good proxy for particulate chloride, and Wang and Hildebrandt Ruiz (2017) observed an average mass ratio of HCl to total organics of 7% for SOA formed from Cl-initiated oxidation of isoprene. (Uptake of HCl onto particulate matter was not found to occur unless the relative humidity of the system was very high, which is not the case here.) In the experiments evaluated here, when Cl was the only oxidant added to the system, the HCl: organic mass ratio ranged from 5 to 10% (Table 1, Fig. S6). This ratio was less than 1% for experiments in which an OH source (HONO or HOOH) was added at the beginning of the experiment, likely due to lower formation of unsaturated products through OH chemistry and/or because a majority of the later-generation products reacted with OH instead of Cl. Overall, the ACSM data suggest that organochlorides form from Cl-initiated oxidation of toluene. The molecular identity or abundance of gas or particle-phase organochlorides cannot be evaluated with the available data – future experiments will utilize iodide as reagent ion in the CIMS to evaluate the molecular identity of gas and particle-phase organochlorides and other oxygenated organics.

SOA formed from Cl-initiated oxidation of toluene was more oxidized than SOA from OH-initiated oxidation of toluene (Fig. 3). Furthermore, while f_{43} of SOA from toluene + OH was relatively high (generally lying to the right hand side (RHS) of the Ng triangle), f_{43} of SOA from toluene + Cl was relatively low (generally lying to the left hand side (LHS) of the triangle) (Ng et al., 2010). OH-initiated oxidation of toluene proceeds primarily via OH-addition to the aromatic ring and is known to form ring-opened products such as butenedial, methyl glyoxal and epoxides (Chhabra et al., 2011). Cl-initiated oxidation of toluene proceeds via H-abstraction at the methyl group and results in ring-retaining products such as benzoquinone, benzaldehyde, benzoic acid, phenol and 1,3,5-benzenetriol. The data presented here are thus consistent with SOA dominated by ring-retaining products (such as SOA from Cl-initiated oxidation of toluene) located on the LHS of the Ng triangle while SOA dominated by ring-opened products (such as SOA from OH-initiated oxidation of toluene) located on the RHS of the Ng triangle. Other researchers have suggested that the presence of methyl groups is associated with higher f_{43} (Li et al., 2016; Sato et al., 2012). Since Cl predominantly reacts with toluene via hydrogen abstraction at the methyl group, leading to aromatic compounds without a methyl group, a lower f_{43} is consistent with this prior work.

Results from the SAPRC model were used to estimate the fraction of toluene reacting with Cl versus with OH as summarized in Table 1. The fraction of toluene reacting with Cl ranged from 0% for experiments in which no source of reactive Cl was added (e.g. Experiments 8 and 9) to 100% for experiments in which no source of OH or NO was added (e.g. Experiment 1, 2 and 5) and included intermediate values of 21% (Expt. 10) and 55% (Expt. 11). In general, f_{43} decreases with the fraction of toluene reacting with Cl consistent with the analysis of the extreme cases (0 and 100%) described above. For experiments in which at least half of the toluene reacts with OH, f_{43} of SOA is similar to experiments in which all toluene reacts with OH. This could suggest that the presence of OH results in a higher abundance of ring-opened higher generation products, regardless of whether the initial oxidation of toluene is by Cl or OH. First and later generation products of toluene oxidation react more quickly with OH than toluene itself. Reaction rates of toluene photo-oxidation products with Cl are unknown; however, this would be consistent with OH oxidation being more important for later-generation chemistry than for the first-generation chemistry, which is also consistent with the analysis of organochloride content presented above. It is also possible that the SAPRC model, which uses a condensed mechanism, underestimates the formation of secondary OH.

3.3. Organic aerosol aging

The complete consumption of toluene in these experiments makes it possible to evaluate the aging of organic aerosol upon continued oxidation. In several experiments, additional oxidant was added after all toluene had reacted with Cl in order to study aging: in Expt. 5, HOOH was added as a low NO_x source of OH (Fig. S7), in Expt. 6 additional Cl_2 was added as a source of Cl (Fig. 4) and in Expt. 7 (Fig. S8), HONO was added as a source of OH and NO_x. The addition of HOOH (low NO_x-OH) in Expt. 5 resulted in a noticeable increase in higher generation gas-phase products but no noticeable change in OA concentrations or bulk composition (f_{43}, f_{44}). The addition of HONO in Expt. 7 resulted in a small increase in OA concentration but no noticeable change in f_{43} or f_{44}. (CIMS data were not available after HONO injection in Expt. 7). The addition of Cl_2 in Expt. 6 resulted in a significant increase in OA, a small decrease in f_{43} and no noticeable change in f_{44}. In terms of gas-phase products, benzaldehyde and phenol decreased upon addition of Cl_2 (Fig. 4), likely because there was no more toluene in the system, so the added Cl reacted with benzaldehyde and phenol to form later generation products. Benzoquinone initially increased but then decreased sharply, likely due to initial formation (from e.g. benzaldehyde, see Fig. S1), followed by continued chemistry. Future work will include measurements of the molecular composition of organic aerosol formed to better observe gas-particle partitioning.

Overall, continued oxidation of the system changes the gas-phase composition and can change OA concentration but does not appear to change bulk OA composition. This may indicate that the system has reached an oxidative end point in the particle phase: Upon further

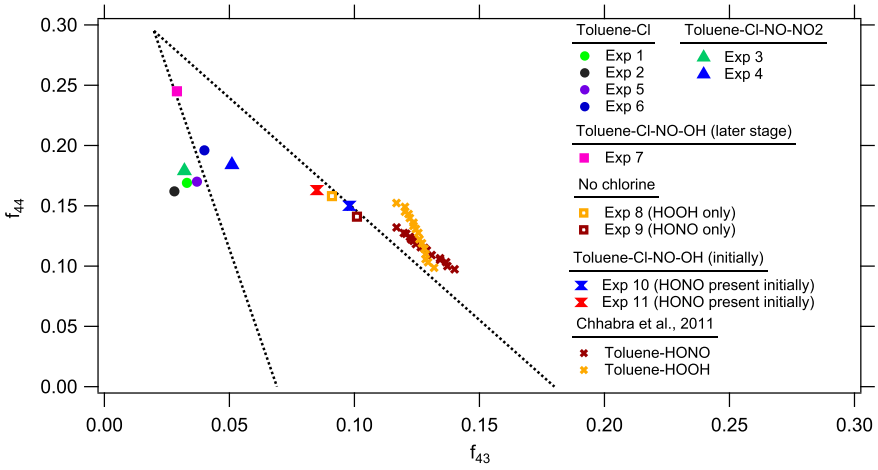

Fig. 3. f_{44} and f_{43} signals as measured by the ACSM in all experiments. The dotted black lines show typical ambient data as reported in Ng et al. (2010).

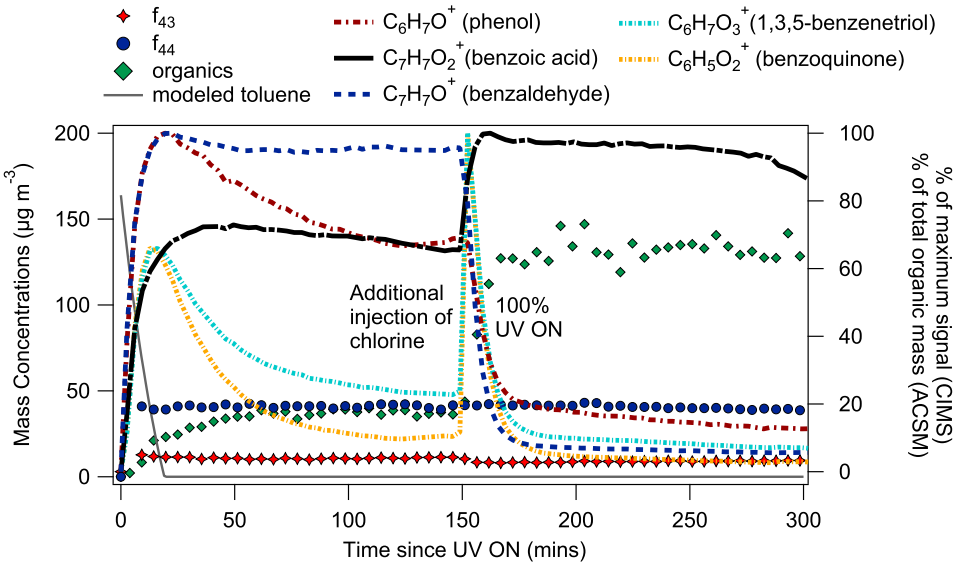

Fig. 4. Time series of wall-loss corrected OA concentration and modeled toluene decay (left vertical axis) and gas-phase products and f_{43}, f_{44} time series (right vertical axis) during experiment 6 (Low NO_x-Cl).

oxidation highly oxidized OA components fragment and partition to the gas-phase - the organic aerosol does not necessarily become more oxygenated according to the bulk OA composition data from the ACSM. Kinetic limitations may play a role on short time scales; however, the bulk OA oxidation state is observed to remain unchanged after UV lights are turned off and the system has had time to equilibrate. Thus, it appears that the OA has reached an oxidative endpoint according to the bulk OA composition data.

4. Conclusions

Chlorine-initiated oxidation of toluene was investigated inside an environmental chamber. Several generations of gas-phase products were observed which followed different qualitative trends in low NO_x and high NO_x environments and responded to the addition of oxidants. SOA formed quickly, and when no source of OH was added to the system initially, all toluene was consumed within less than 30 min of oxidation, enabling the investigation of organic aerosol aging. SOA concentrations remained stable upon continued exposure to UV suggesting that most semi-volatile products are not photo-labile. The bulk OA composition depends on the initiating radical: Cl-initiated oxidation of toluene forms SOA with an overall higher oxidation state and lower fraction of organic signal due to ions at m/z 43 (f_{43}). These differences are probably due to the approximately 10-fold faster reaction timescales of toluene with Cl than with OH, and the predominance of ring-retaining products without methyl groups in the toluene + Cl system. Addition of oxidant (Cl_2, HOOH or HONO) after all toluene was consumed did not change the organic aerosol oxidation state, suggesting an oxidative end-point in the particle phase.

SOA formation from Cl-initiated oxidation of hydrocarbons including toluene may significantly impact tropospheric composition considering that concentrations of reactive chlorine species are higher than previously assumed, and that Cl reacts more quickly than OH with most hydrocarbons. For example, this work suggests that when Cl concentrations are a factor of 10 lower than OH concentrations, Cl and OH-initiated oxidation of toluene contribute similarly to the formation of toluene SOA. The faster reaction rate also enables complete precursor consumption and investigation of aging reactions on common experimental timescales. In addition to its relevance to tropospheric composition, chlorine chemistry could thus be important as an experimental tool.

Data availability

Data published in this paper's figures and tables are available via the Texas Data Repository, https://doi.org/10.18738/T8/IPOEGR. Underlying research data are also available by request to Lea Hildebrandt Ruiz: lhr@che.utexas.edu.

CRediT authorship contribution statement

Surya Venkatesh Dhulipala: Data curation, Formal analysis, Investigation, Methodology, Validation, Visualization, Writing – original draft, Writing – review & editing. **Sahil Bhandari:** Data curation, Formal analysis, Investigation, Methodology, Writing – original draft, Writing – review & editing. **Lea Hildebrandt Ruiz:** Conceptualization, Formal analysis, Funding acquisition, Investigation, Methodology, Project administration, Resources, Supervision, Validation, Visualization, Writing – original draft, Writing – review & editing.

Acknowledgements

This projected was supported by the National Science Foundation Grant No. 1653625 and by the Welch Foundation Grant No. F-1925.

Appendix A. Supplementary data

Supplementary data to this article can be found online at https://doi.org/10.1016/j.atmosenv.2018.11.002.

References

Aiken, A.C., DeCarlo, P.F., Jimenez, J.L., 2007. Elemental analysis of organic species with electron ionization high-resolution mass spectrometry. Anal. Chem. 79, 8350–8358. https://doi.org/10.1021/ac071150w.

Aiken, A.C., Decarlo, P.F., Kroll, J.H., Worsnop, D.R., Alex Huffman, J., Docherty, K.S., Ulbrich, I.M., Mohr, C., Kimmel, J.R., Sueper, D., Sun, Yele, Zhang, Q., Trimborn, A., Northway, M., Ziemann, P.J., Canagaratna, M.R., Onasch, T.B., Alfarra, M.R., Prevot, A.S.H., Dommen, J., Duplissy, J., Metzger, A., Baltensperger, U., Jimenez, J.L., 2008. O/C and OM/OC ratios of primary, secondary, and ambient organic aerosols with high resolution time-of-flight aerosol mass spectrometry. Environ. Sci. Technol. 42, 4478–4485. https://doi.org/10.1021/es703009q.

Aljawhary, D., Lee, A.K.Y., Abbatt, J.P.D., 2013. High-resolution chemical ionization mass spectrometry (ToF-CIMS): application to study SOA composition and processing. Atmos. Meas. Tech. 6, 3211–3224. https://doi.org/10.5194/amt-6-3211-2013.

Allan, J.D., Delia, A.E., Coe, H., Bower, K.N., Worsnop, D.R., 2004. A generalised method

for the extraction of chemically resolved mass spectra from Aerodyne aerosol mass spectrometer data. J. Aerosol Sci. 35, 909–922. https://doi.org/10.1016/j.jaerosci.2004.02.007.

Alramadan, A.S., Sarathy, S.M., Khurshid, M., Badra, J., 2016. A blending rule for octane numbers of PRFs and TPRFs with ethanol. Fuel 180, 175–186. https://doi.org/10.1016/j.fuel.2016.04.032.

Behnke, W., George, C., Scheer, V., Zetzsch, C., 1997. Production and decay of ClNO2 from the reaction of gaseous N2O 5 with NaCl solution: bulk and aerosol experiments. J. Geophys. Res. Atmos. 102, 3795–3804. https://doi.org/10.1029/96JD03057.

Bertram, T.H., Kimmel, J.R., Crisp, T.A., Ryder, O.S., Yatavelli, R.L.N., Thornton, J.A., Cubison, M.J., Gonin, M., Worsnop, D.R., 2011. A field-deployable, chemical ionization time-of-flight mass spectrometer. Atmos. Meas. Tech. 4, 1471–1479. https://doi.org/10.5194/amt-4-1471-2011.

Birdsall, A.W., Andreoni, J.F., Elrod, M.J., 2010. Investigation of the role of bicyclic peroxy radicals in the oxidation mechanism of toluene. J. Phys. Chem. 114, 10655–10663. https://doi.org/10.1021/jp105467e.

Birdsall, A.W., Elrod, M.J., 2011. Comprehensive NO-dependent study of the products of the oxidation of atmospherically relevant aromatic compounds. J. Phys. Chem. 115, 5397–5407. https://doi.org/10.1021/jp2010327.

Brook, R.D., Rajagopalan, S., Iii, C.A.P., Brook, J.R., Bhatnagar, A., Diez-roux, A.V., Holguin, F., Hong, Y., Luepker, R.V., Mittleman, M.A., Peters, A., Siscovick, D., Smith, S.C., Whitsel, L., Kaufman, J.D., 2016. Particulate matter air pollution and cardiovascular disease. Circulation 121, 2331–2378. https://doi.org/10.1161/CIR.0b013e3181dbece1.

Cai, X., Ziemba, L.D., Griffin, R.J., 2008. Secondary Aerosol Formation from the Oxidation of Toluene by Chlorine Atoms. Atmospheric Environmenthttps://doi.org/10.1016/j.atmosenv.2008.07.014.

Calvert, J.G., Atkinson, R., Becker, K.H., Kamens, R.M., Seinfeld, J.H., Wallington, T.H., Yarwood, G., 2002. In: The Mechanisms of Atmospheric Oxidation of the Aromatic Hydrocarbons, first ed. Oxford University Press, New York.

Canagaratna, M.R., Jimenez, J.L., Kroll, J.H., Chen, Q., Kessler, S.H., Massoli, P., Hildebrandt Ruiz, L., Fortner, E., Williams, L.R., Wilson, K.R., Surratt, J.D., Donahue, N.M., Jayne, J.T., Worsnop, D.R., 2015. Elemental ratio measurements of organic compounds using aerosol mass spectrometry: characterization, improved calibration, and implications. Atmos. Chem. Phys. 15, 253–272. https://doi.org/10.5194/acp-15-253-2015.

Carter, W.P.L., Cocker, D.R., Fitz, D.R., Malkina, I.L., Bumiller, K., Sauer, C.G., Pisano, J.T., Bufalino, C., Song, C., 2005. A new environmental chamber for evaluation of gas-phase chemical mechanisms and secondary aerosol formation. Atmos. Environ. 39, 7768–7788. https://doi.org/10.1016/j.atmosenv.2005.08.040.

Carter, W.P.L., Heo, G., 2013. Development of revised SAPRC aromatics mechanisms. Atmos. Environ. 77, 404–414. https://doi.org/10.1016/j.atmosenv.2013.05.021.

Chang, C.T., Liu, T.H., Jeng, F.T., 2004. Atmospheric concentrations of the Cl atom, ClO radical, and HO radical in the coastal marine boundary layer. Environ. Res. 94, 67–74. https://doi.org/10.1016/j.envres.2003.07.008.

Chang, S., Allen, D.T., 2006. Chlorine chemistry in urban atmospheres: aerosol formation associated with anthropogenic chlorine emissions in southeast Texas. Atmos. Environ. 40, 512–523. https://doi.org/10.1016/j.atmosenv.2006.04.070.

Chhabra, P.S., Ng, N.L., Canagaratna, M.R., Corrigan, A.L., Russell, L.M., Worsnop, D.R., Flagan, R.C., Seinfeld, J.H., 2011. Elemental composition and oxidation of chamber organic aerosol. Atmos. Chem. Phys. 11, 8827–8845. https://doi.org/10.5194/acp-11-8827-2011.

Cohen, A.J., Brauer, M., Burnett, R., Anderson, H.R., Frostad, J., Estep, K., Balakrishnan, K., Brunekreef, B., Dandona, L., Dandona, R., Feigin, V., Freedman, G., Hubbell, B., Jobling, A., Kan, H., Knibbs, L., Liu, Y., Martin, R., Morawska, L., Pope, C.A., Shin, H., Straif, K., Shaddick, G., Thomas, M., van Dingenen, R., van Donkelaar, A., Vos, T., Murray, C.J.L., Forouzanfar, M.H., 2017. Estimates and 25-year trends of the global burden of disease attributable to ambient air pollution: an analysis of data from the Global Burden of Diseases Study 2015. Lancet 389, 1907. https://doi.org/10.1016/S0140-6736(17)30505-6.

Cubison, M.J., Jimenez, J.L., 2015. Statistical precision of the intensities retrieved from constrained fitting of overlapping peaks in high-resolution mass spectra. Atmos. Meas. Tech. 8, 2333–2345. https://doi.org/10.5194/amt-8-2333-2015.

de Gouw, J., Warneke, C., 2007. Measurements of volatile organic compounds in the earth's atmosphere using proton-transfer-reaction mass spectrometry. Mass Spectrom. Rev. 26, 223–257. https://doi.org/10.1002/mas.20119.

Diehl, J.W., Di Sanzo, F.P., 2005. Determination of aromatic hydrocarbons in gasolines by flow modulated comprehensive two-dimensional gas chromatography. J. Chromatogr. A 1080, 157–165. https://doi.org/10.1016/j.chroma.2004.11.054.

Fabri, J., Graeser, U., Simo, T.A., 2000. Toluene. Ullmann's Encyclopedia of Industrial Chemistry. https://doi.org/10.1002/14356007.a27_147.pub2.

Fantechi, G., Jensen, N.R., Saastad, O.L.E., Hjorth, J., Peeters, J., 1998. Reactions of Cl atoms with selected VOCs: kinetics, products and mechanisms. J. Atmos. Chem. 31, 247–267. https://doi.org/10.1023/A:1006033910014.

Faxon, C.B., Allen, D.T., 2013. Chlorine chemistry in urban atmospheres: a review. Environ. Chem. 10, 221–233. https://doi.org/10.1071/EN13026.

Faxon, C.B., Dhulipala, S.V., Allen, D.T., Hildebrandt Ruiz, L., 2018. Heterogeneous production of Cl2 from particulate chloride: effects of composition and relative humidity. AIChE J. 64, 3151–3158. https://doi.org/10.1002/aic.16204.

Finlayson-Pitts, B.J., 1993. Chlorine atoms as a potential tropospheric oxidant in the marine boundary layer. Res. Chem. Intermed. 19, 235–249. https://doi.org/10.1163/156856793X00091.

Finlayson-Pitts, B.J., Ezell, M.J., Pitts Jr., J.N., 1989. Formation of chemically active chlorine compounds by reactions of atmospheric NaCl particles with gaseous N2O5 and ClONO2. Nature 337, 241–244. https://doi.org/10.1038/337241a0.

Fortner, E.C., Zheng, J., Zhang, R., Berk Knighton, W., Volkamer, R.M., Sheehy, P., Molina, L., Andŕe, M., 2009. Measurements of volatile organic compounds using proton transfer reaction-mass spectrometry during the MILAGRO 2006 campaign. Atmos. Chem. Phys. 9, 467–481. https://doi.org/10.5194/acp-9-467-2009.

Graedel, T.E., Keene, W.C., 1995. Tropospheric budget of reactive chlorine. Global Biogeochem. Cycles 9, 47–77. https://doi.org/10.1029/94GB03103.

Hallquist, M., Wenger, J.C., Baltensperger, U., Rudich, Y., Simpson, D., Claeys, M., Dommen, J., Donahue, N.M., George, C., Goldstein, A.H., Hamilton, J.F., Herrmann, H., Hoffmann, T., Iinuma, Y., Jang, M., Jenkin, M.E., Jimenez, J.L., Kiendler-Scharr, A., Maenhaut, W., McFiggans, G., Mentel, Th F., Monod, A., Prévôt, A.S.H., Seinfeld, J.H., Surratt, J.D., Szmigielski, R., Wildt, J., 2009. The formation, properties and impact of secondary organic aerosol: current and emerging issues. Atmos. Chem. Phys. 9, 5155–5236. https://doi.org/10.5194/acp-9-5155-2009.

Hamra, G.B., Guha, N., Cohen, A., Laden, F., Raaschou-Nielsen, O., Samet, J.M., Vineis, P., Forastiere, F., Saldiva, P., Yorifuji, T., Loomis, D., 2014. Outdoor particulate matter exposure and lung Cancer : a systematic review and meta-analysis. Environ. Health Perspect. 906–911. https://doi.org/10.1289/ehp.122-A294.

Heald, C.L., Kroll, J.H., Jimenez, J.L., Docherty, K.S., DeCarlo, P.F., Aiken, A.C., Chen, Q., Martin, S.T., Farmer, D.K., Artaxo, P., 2010. A simplified description of the evolution of organic aerosol composition in the atmosphere. Geophys. Res. Lett. 37, L08803. https://doi.org/10.1029/2010GL042737.

Hildebrandt, L., Donahue, N.M., Pandis, S.N., 2009. High formation of secondary organic aerosol from the photo-oxidation of toluene. Atmos. Chem. Phys. 9, 2973–2986. https://doi.org/10.5194/acp-9-2973-2009.

Hildebrandt Ruiz, L., Paciga, A.L., Cerully, K.M., Nenes, A., Donahue, N.M., Pandis, S.N., 2015. Formation and aging of secondary organic aerosol from toluene: changes in chemical composition, volatility, and hygroscopicity. Atmos. Chem. Phys. 15, 8301–8313. https://doi.org/10.5194/acp-15-8301-2015.

Huang, M., Liu, X., Hu, C., Guo, X., Gu, X., Zhao, W., Wang, Z., Fang, L., Zhang, W., 2014. Aerosol laser time-of-flight mass spectrometer for the on-line measurement of secondary organic aerosol in smog chamber. Meas. J. Int. Meas. Confed. 55, 394–401. https://doi.org/10.1016/j.measurement.2014.05.038.

Huang, M., Zhang, W., Gu, X., Hu, C., Zhao, W., Wang, Z., Fang, L., 2012. Size distribution and chemical composition of secondary organic aerosol formed from Cl-initiated oxidation of toluene. J. Environ. Sci. 24, 860–864. https://doi.org/10.1016/S1001-0742(11)60840-1.

Jimenez, J.L., Canagaratna, M.R., Donahue, N.M., Prevot, A.S.H., Zhang, Q., Kroll, J.H., DeCarlo, P.F., Allan, J.D., Coe, H., Ng, N.L., Aiken, A.C., Docherty, K.S., Ulbrich, I.M., Grieshop, A.P., Robinson, A.L., Duplissy, J., Smith, J.D., Wilson, K.R., Lanz, V.A., Hueglin, C., Sun, Y.L., Tian, J., Laaksonen, A., Raatikainen, T., Rautiainen, J., Vaattovaara, P., Ehn, M., Kulmala, M., Tomlinson, J.M., Collins, D.R., Cubison, M.J., Dunlea, E.J., Huffman, J.A., Onasch, T.B., Alfarra, M.R., Williams, P.I., Bower, K., Kondo, Y., Schneider, J., Drewnick, F., Borrmann, S., Weimer, S., Demerjian, K., Salcedo, D., Cottrell, L., Griffin, R., Takami, A., Miyoshi, T., Hatakeyama, S., Shimono, A., Sun, J.Y., Zhang, Y.M., Dzepina, K., Kimmel, J.R., Sueper, D., Jayne, J.T., Herndon, S.C., Trimborn, A.M., Williams, L.R., Wood, E.C., Middlebrook, A.M., Kolb, C.E., Baltensperger, U., Worsnop, D.R., 2009. Evolution of organic aerosols in the atmosphere. Science 84 326, 1525–1529. https://doi.org/10.1126/science.1180353.

Kampa, M., Castanas, E., 2008. Human health effects of air pollution. Environ. Pollut. 151, 362–367. https://doi.org/10.1016/j.envpol.2007.06.012.

Karlsson, R.S., Szente, J.J., Ball, J.C., Maricq, M.M., 2001. Homogeneous aerosol formation by the chlorine atom initiated oxidation of toluene. J. Phys. Chem. 105, 82–96. https://doi.org/10.1021/jp001831u.

Kebabian, P.L., Wood, E.C., Herndon, S.C., Freedman, A., 2008. A practical alternative to chemiluminescence-based detection of nitrogen dioxide: cavity attenuated phase shift spectroscopy. Environ. Sci. Technol. 42, 6040–6045. https://doi.org/10.1021/es703204j.

Kroll, J.H., Smith, J.D., Che, D.L., Kessler, D.S.H., Worsnop, D.R., Wilson, K.R., 2009. Measurement of fragmentation and functionalization pathways in the heterogeneous oxidation of oxidized organic aerosol. Phys. Chem. Chem. Phys. 11, 8005–8014. https://doi.org/10.1039/b905289e.

Lee, B.H., Lopez-Hilfiker, F.D., Mohr, C., Kurtén, T., Worsnop, D.R., Thornton, J. a, 2014. An iodide-adduct high-resolution time-of-flight chemical-ionization mass spectrometer: application to atmospheric inorganic and organic compounds. Environ. Sci. Technol. 48, 6309–6317. https://doi.org/10.1021/es500362a.

Li, L., Tang, P., Nakao, S., Chen, C., Iii, D.R.C., 2016. Role of methyl group number on SOA formation from monocyclic aromatic hydrocarbons photooxidation under low-NOx conditions. Atmos. Chem. Phys. 2255–2272. https://doi.org/10.5194/acp-16-2255-2016.

Mallik, C., Tomsche, L., Bourtsoukidis, E., Crowley, J.N., Derstroff, B., Fischer, H., Hafermann, S., Hueser, I., Javed, U., Kessel, S., Lelieveld, J., Martinez, M., Meusel, H., Novelli, A., Phillips, G.J., Pozzer, A., Reiffs, A.5, Sander, R., Taraborrelli, D., Sauvage, C., Schuladen, J., Su, H., Williams, J., Harder, H., 2018. Oxidation Processes in the Eastern Mediterranean Atmosphere: Evidence from the Modelling of HOx Measurements over Cyprus. pp. 1–35. https://doi.org/10.5194/acp-2018-25.

Molina, M.J., Zhang, R., Broekhuizen, K., Lei, W., Navarro, R., Molina, L.T., 1999. Experimental study of intermediates from OH-initiated reactions of toluene [8]. J. Am. Chem. Soc. 121, 10225–10226. https://doi.org/10.1021/ja992461u.

Ng, N.L., Canagaratna, M.R., Zhang, Q., Jimenez, J.L., Tian, J., Ulbrich, I.M., Kroll, J.H., Docherty, K.S., Chhabra, P.S., Bahreini, R., Murphy, S.M., Seinfeld, J.H., Hildebrandt, L., Donahue, N.M., Decarlo, P.F., Lanz, V.A., Prévôt, A.S.H., Dinar, E., Rudich, Y., Worsnop, D.R., 2010. Organic aerosol components observed in northern hemispheric datasets from aerosol mass spectrometry. Atmos. Chem. Phys. 10, 4625–4641. https://doi.org/10.5194/acp-10-4625-2010.

Ng, N.L., Herndon, S.C., Trimborn, A., Canagaratna, M.R., Croteau, P.L., Onasch, T.B., Sueper, D., Worsnop, D.R., Zhang, Q., Sun, Y.L., Jayne, J.T., 2011. An Aerosol

Chemical Speciation Monitor (ACSM) for routine monitoring of the composition and mass concentrations of ambient aerosol. Aerosol Sci. Technol. 45, 770–784. https://doi.org/10.1080/02786826.2011.560211.

Ng, N.L., Kroll, J.H., Chan, A.W.H., Chhabra, P.S., Flagan, R.C., Seinfeld, J.H., 2007. Secondary organic aerosol formation from *m*-xylene, toluene, and benzene. Atmos. Chem. Phys. 7, 3909–3922. https://doi.org/10.5194/acp-7-3909-2007.

Noda, J., Volkamer, R., Molina, M.J., 2009. Dealkylation of alkylbenzenes: a significant pathway in the toluene, o-, m-, p-xylene + OH reaction. J. Phys. Chem. 113, 9658–9666. https://doi.org/10.1021/jp901529k.

Pankow, J.F., 1994. An absorption model of the gas/aerosol partioning involved in the formation of secondary organic aerosol. Atmos. Environ. 28, 189–193. https://doi.org/10.1016/1352-2310(94)90094-9.

Peng, R.D., Chang, H.H., Bell, M.L., McDermott, A., Zeger, S.L., Samet, J.M., Dominici, F., 2008. Coarse particulate matter air pollution and hospital admissions for cardiovascular and respiratory diseases among Medicare patients. J. Am. Med. Assoc. 299 (18), 2172–2179. https://doi.org/10.1001/jama.299.18.2172.

Poschl, U., 2005. Atmospheric aerosols: composition, transformation, climate and health effects. Angew. Chem. Int. Ed. 44, 7520–7540. https://doi.org/10.1002/anie.200501122.

Robinson, A.L., Donahue, N.M., Shrivastava, M.K., Weitkamp, E.A., Sage, A.M., Grieshop, A.P., Lane, T.E., Pierce, J.R., Pandis, S.N., 2007. Rethinking organic aerosols: semivolatile emissions and photochemical aging. Science 315, 1259–1262. https://doi.org/10.1126/science.1133061.

Rudich, Y., Donahue, N.M., Mentel, T.F., 2007. Aging of organic aerosol: bridging the gap between laboratory and field studies. Annu. Rev. Phys. Chem. 58, 321–352. https://doi.org/10.1146/annurev.physchem.58.032806.104432.

Sarwar, G., Simon, H., Bhave, P., Yarwood, G., 2012. Examining the impact of heterogeneous nitryl chloride production on air quality across the United States. Atmos. Chem. Phys. 12, 6455–6473. https://doi.org/10.5194/acp-12-6455-2012.

Sato, K., Takami, A., Kato, Y., Seta, T., Fujitani, Y., Hikida, T., Shimono, A., Imamura, T., 2012. Physics AMS and LC/MS analyses of SOA from the photooxidation of benzene and 1,3,5-trimethylbenzene in the presence of NOx: effects of chemical structure on SOA aging. Atmos. Chem. Phys. 12, 4667–4682. https://doi.org/10.5194/acp-12-4667-2012.

Saxena, P., Hildemann, L.M., 1996. Water-soluble organics in atmospheric Particles : a critical review of the literature and application of thermodynamics to identify candidate compounds. J. Atmos. Chem. 24, 57–109. https://doi.org/10.1007/BF00053823.

Shrivastava, M.K., Lane, T.E., Donahue, N.M., Pandis, S.N., Robinson, A.L., 2008. Effects of gas particle partitioning and aging of primary emissions on urban and regional organic aerosol concentrations. J. Geophys. Res. 113, D18301. https://doi.org/10.1029/2007JD009735.

Spicer, C.W., Chapman, E.G., Finlayson-Pitts, B.J., Plastridge, R.A., Hubbe, J.M., Fast, J.D., Berkowitz, C.M., 1998. Unexpectedly high concentrations of molecular chlorine in coastal air. Nature 394, 353–356. https://doi.org/10.1038/28584.

Suh, I., Zhang, D., Zhang, R., Molina, L.T., Molina, M.J., 2002. Theoretical study of OH addition reaction to toluene. Chem. Phys. Lett. 364, 454–462. https://doi.org/10.1016/S0009-2614(02)01364-7.

Suh, I., Zhang, R., Molina, L.T., Molina, M.J., 2003. Oxidation mechanism of aromatic peroxy and bicyclic radicals from OH-toluene reactions. J. Am. Chem. Soc. 125, 12655–12665. https://doi.org/10.1021/ja0350280.

Tanaka, P.L., Oldfield, S., Neece, J.D., Mullins, C.B., 2000. Anthropogenic Sources of Chlorine and Ozone Formation in Urban Atmospheres 34. pp. 4470–4473. https://doi.org/10.1021/es991380v.

Wang, D.S., Hildebrandt Ruiz, L., 2017. Secondary organic aerosol from chlorine-initiated oxidation of isoprene. Atmos. Chem. Phys. 17, 13491–13508. https://doi.org/10.5194/acp-17-13491-2017.

Wang, L., Arey, J., Atkinson, R., 2005. Reactions of chlorine atoms with a series of aromatic hydrocarbons. Environ. Sci. Technol. 39, 5302–5310. https://doi.org/10.1021/es0479437.

Wang, M., Zhu, T., Zheng, J., Zhang, R.Y., Zhang, S.Q., Xie, X.X., Han, Y.Q., Li, Y., 2009. Use of a mobile laboratory to evaluate changes in on-road air pollutants during the Beijing 2008 summer olympics. Atmos. Chem. Phys. 9, 8247–8263. https://doi.org/10.5194/acp-9-8247-2009.

Winer, A.M., Peters, J.W., Smith, J.P., Pitts, J.N., 1974. Response of commercial chemiluminescent NO-NO2analyzers to other nitrogen-containing compounds. Environ. Sci. Technol. 8, 1118–1121. https://doi.org/10.1021/es60098a004.

Yarwood, G., Whitten, G.Z., Jung, J., Heo, G., Allen, D.T., 2010. Development, Evaluation and Testing of Version 6 of the Carbon Bond Chemical Mechanism (CB6).

Yatavelli, R.L.N., Lopez-Hilfiker, F., Wargo, J.D., Kimmel, J.R., Cubison, M.J., Bertram, T.H., Jimenez, J.L., Gonin, M., Worsnop, D.R., Thornton, J. a., 2012. A chemical ionization high-resolution time-of-flight mass spectrometer coupled to a micro orifice volatilization impactor (MOVI-HRToF-CIMS) for analysis of gas and particle-phase organic species. Aerosol Sci. Technol. 46, 1313–1327. https://doi.org/10.1080/02786826.2012.712236.

Young, C.J., Washenfelder, R.A., Edwards, P.M., Parrish, D.D., Gilman, J.B., Kuster, W.C., Mielke, L.H., Osthoff, H.D., Tsai, C., Pikelnaya, O., Stutz, J., Veres, P.R., Roberts, J.M., Griffith, S., Dusanter, S., Stevens, P.S., Flynn, J., Grossberg, N., Lefer, B., Holloway, J.S., Peischl, J., Ryerson, T.B., Atlas, E.L., Blake, D.R., Brown, S.S., 2014. Chlorine as a primary radical: evaluation of methods to understand its role in initiation of oxidative cycles. Atmos. Chem. Phys. 14, 3427–3440. https://doi.org/10.5194/acp-14-3427-2014.

Zhang, Z., Lin, L., Wang, L., 2012. Atmospheric oxidation mechanism of naphthalene initiated by OH radical. A theoretical study. Phys. Chem. Chem. Phys. 14, 2645–2650. https://doi.org/10.1039/c2cp23271e.

Supplementary Information for "Formation of oxidized organic compounds from Cl-initiated oxidation of toluene"

Surya Venkatesh Dhulipala, Sahil Bhandari and Lea Hildebrandt Ruiz

McKetta Department of Chemical Engineering, The University of Texas at Austin, Austin, TX 78712, USA; svd@utexas.edu (S.V.D); sahilb@utexas.edu (S.B.)

Correspondence to: Lea Hildebrandt Ruiz (lhr@che.utexas.edu); Tel.: +1-512-471-1050

S1. Environmental chamber characterization experiments

The following characterization experiments were conducted based on procedures published in Carter et al. (2005):

1) Light Characterization: The intensity of the UV lights was characterized by the photolysis rate of NO_2, which was measured to be 0.3 min^{-1} when all UV lights are used, similar to ambient NO_2 photolysis rates (e.g., 0.46 min^{-1} at a zenith angle of 40, Carter et al., 2005).
2) Leak Rate Characterization: Leak rates were estimated by injecting a tracer species such as N_2 and Cl_2 into the environmental chamber and observing their leak rate over 6-10 hours. UV Lights were turned off during this test. The corresponding value was 0.29 ppb min^{-1}, determined experimentally and also verified using the SAPRC CB6R5 model.
3) HONO off-gassing from chamber walls: The SAPRC CB6R5 modeled value of HONO off-gassing rate was 11.14 ppt min^{-1}. The ratio of the HONO off-gassing rate relative to the NO_2 photolysis rate was 0.032 ppb.
4) HCHO off-gasing from chamber walls: The SAPRC CB6R5 modeled value of the ratio of HCHO off-gasing rate relative to the NO_2 photolysis rate was 0.6 ppb.

Tables and Figures

The Benzyl Creigee Intermediate (Figure S1) is known to undergo multiple stages of oxidation in the presence of Cl to form several products including phenyl hydroperoxide, benzoic acid, perbenzoic acid, 1,4-benzoquinone, phenol and phenyl hydroperoxide. Some of these products are also known to be minor products of toluene-OH chemistry.

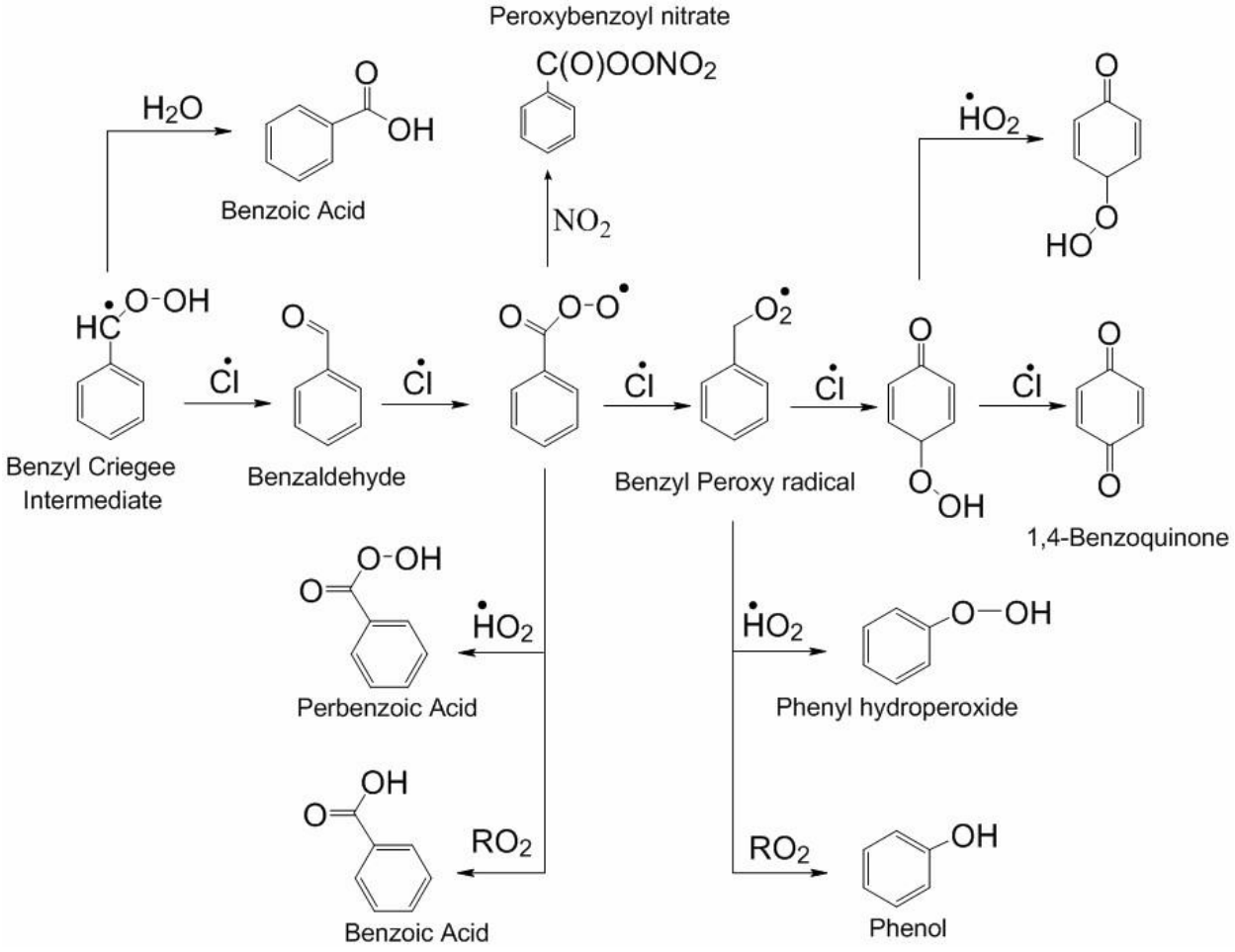

Figure S1. Continued oxidation of Benzyl Criegee intermediate modified from several sources (Cai et al., 2008; Fantechi et al., 1998; Huang et al., 2014, 2012; Karlsson et al., 2001; Wang et al., 2005; Young et al., 2014).

Table S1. Availability of instruments (Y = yes, N = no)

Exp.	SEMS	ACSM	CIMS	Ozone monitor	NO_x monitor	NO_2 monitor
1	Y	Y	Y	Y	Y	N
2	Y	Y	Y	Y	Y	N
3	Y	Y	Y	N	Y	N
4	Y	Y	Y	N	Y	N
5	Y	Y	Y	N	N	N
6	Y	Y	Y	Y	N	N
7	Y	Y	Y	Y	Y	N
8	Y	Y	Y	N	N	N
9	Y	Y	Y	Y	Y	Y
10	Y	Y	Y	Y	Y	Y
11	Y	Y	Y	Y	Y	Y

Table S2. Modeled concentratiosn of OH, Cl and $ClNO_2$, 5 min after UV lights on.

Exp	[OH·] (molecules cm^{-3})	[Cl·] (molecules cm^{-3})	[$ClNO_2$] (ppb)
1	7.91×10^{4}	2.27×10^{7}	N/A
2	1.70×10^{5}	1.94×10^{8}	N/A
3	2.20×10^{7}	1.06×10^{8}	2.00
4	2.80×10^{7}	1.97×10^{7}	0.59
5	1.58×10^{5}	1.41×10^{8}	N/A
6	8.59×10^{4}	2.58×10^{7}	N/A
7	1.03×10^{7}	1.43×10^{8}	1.27
8	1.46×10^{6}	N/A	N/A
9	5.94×10^{7}	N/A	N/A
10	5.56×10^{7}	2.93×10^{6}	1.55
11	4.04×10^{7}	3.75×10^{6}	1.52

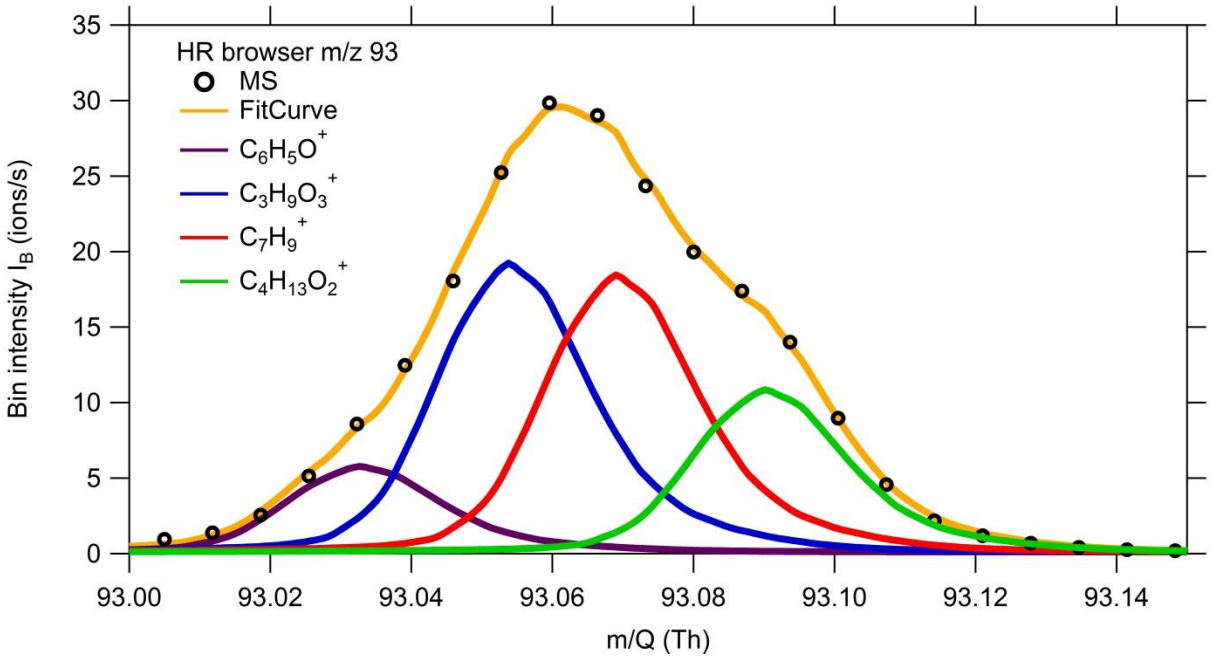

Figure S2. HR-Tof-CIMS mass spectrum (30 minute average) after lights were turned off during experiment 1. Toluene could not be quantified reliably due to the presence of four nearby peaks at *m/z* 93 (Cubison and Jimenez, 2015): $C_6H_5O^+$, $C_3H_9O_3^+$, $C_7H_9^+$, and $C_4H_{13}O_2^+$.

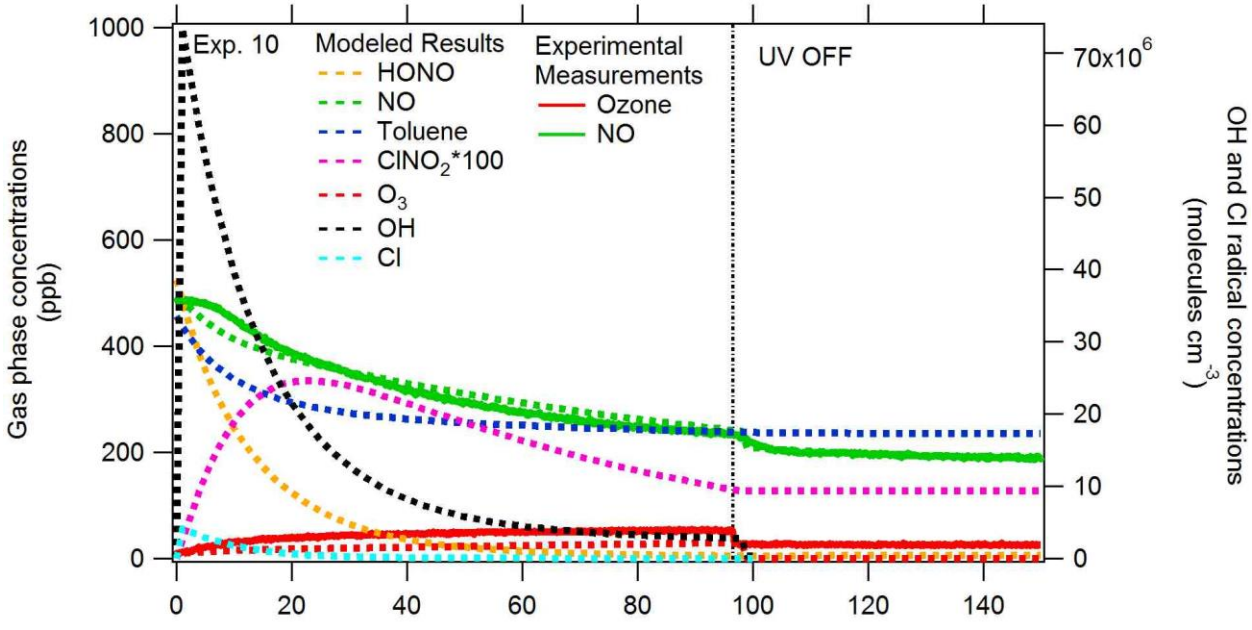

Figure S3. Time series of experimental measurements and modeled results for gas-phase species during experiment 10.

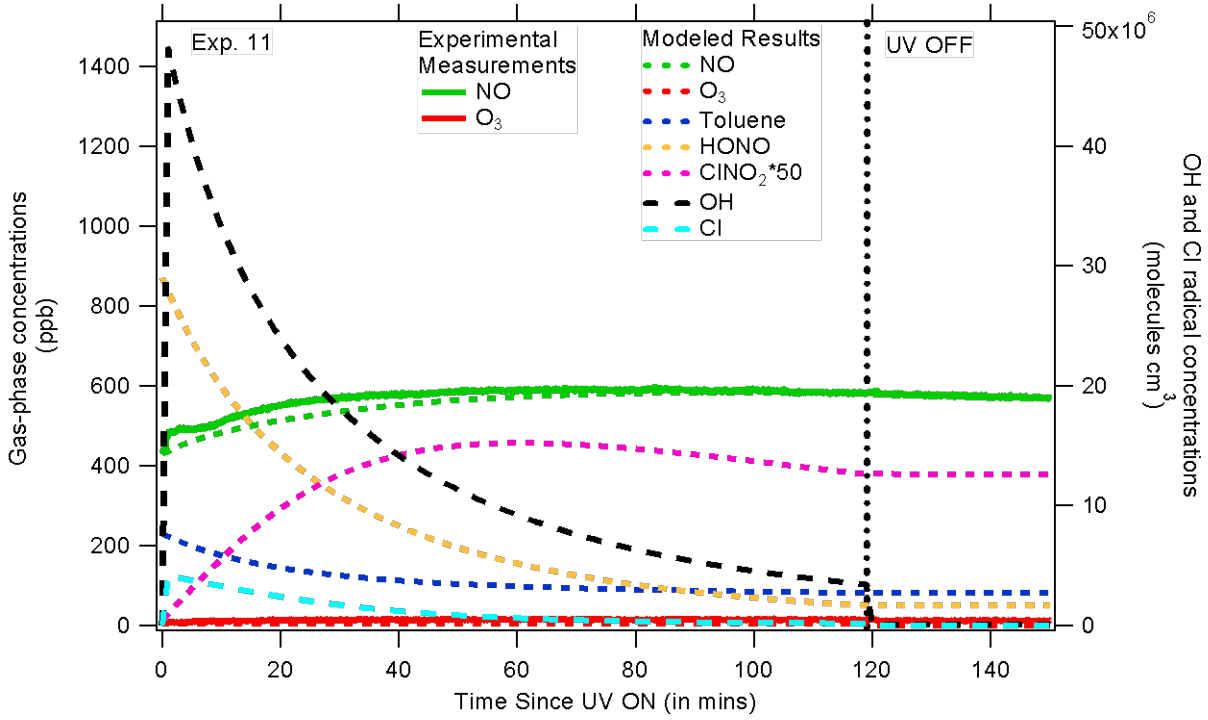

Figure S4. Time series of experimental measurements and modeled results for gas-phase species during experiment 11.

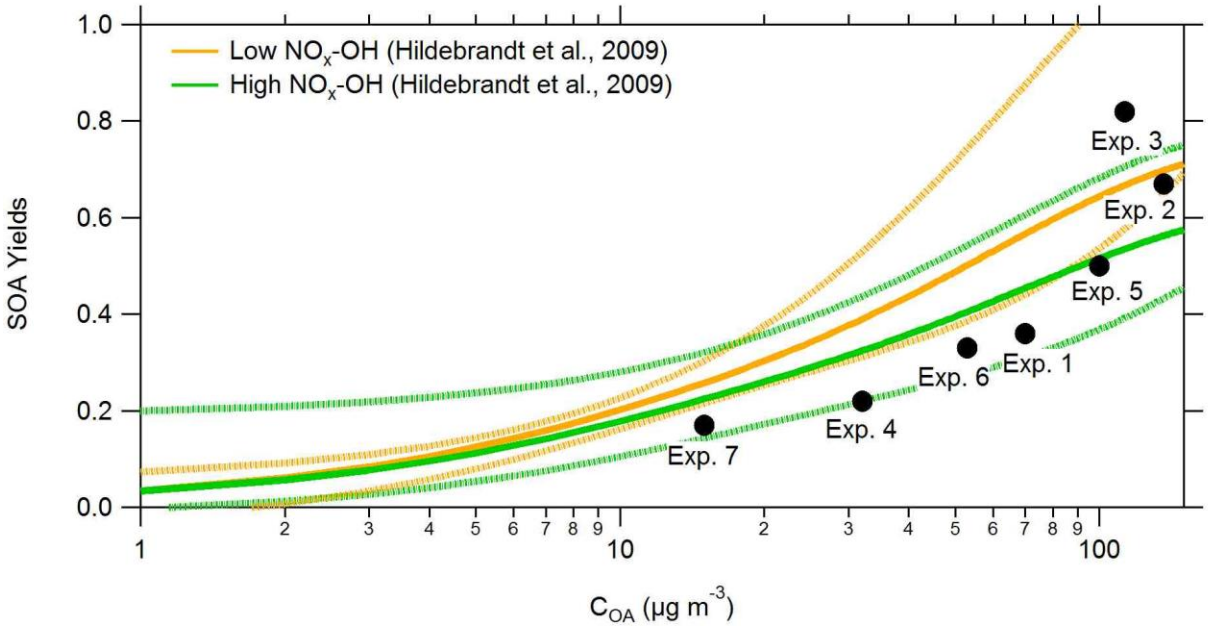

Figure S5. SOA yields as a function of total organic mass concentration in the environmental chamber for experiments 1-7. SOA yields were only calculated for experiments where modeling results suggested complete consumption of toluene. Dotted lines represent upper and lower bounds for low NO_x-OH (orange) and high NO_x-OH (green) from Hildebrandt et al., 2009.

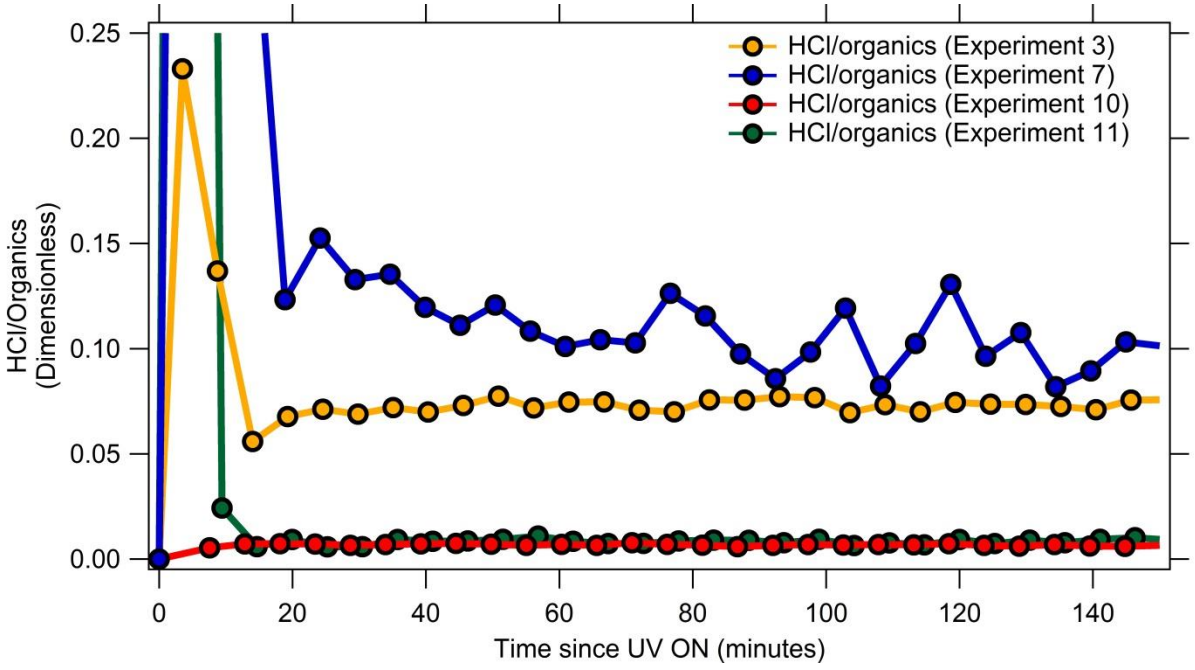

Figure S6. Time series of particulate HCl over organics over duration of experiment 3, 7, 10 and 11.

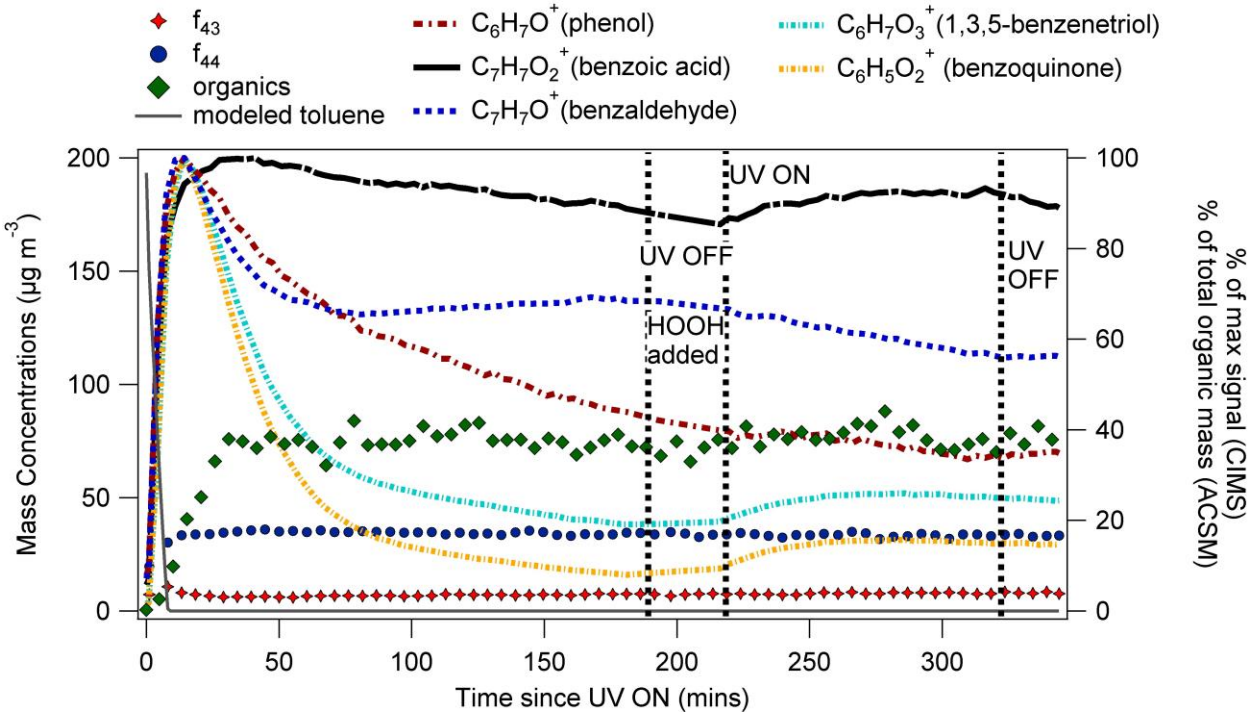

Figure S7. Time series of wall-loss corrected OA concentration and modeled toluene decay (left vertical axis), and gas-phase products and f_{43}, f_{44} (right vertical axis) during experiment 5 (Low NO_x-Cl-HOOH).

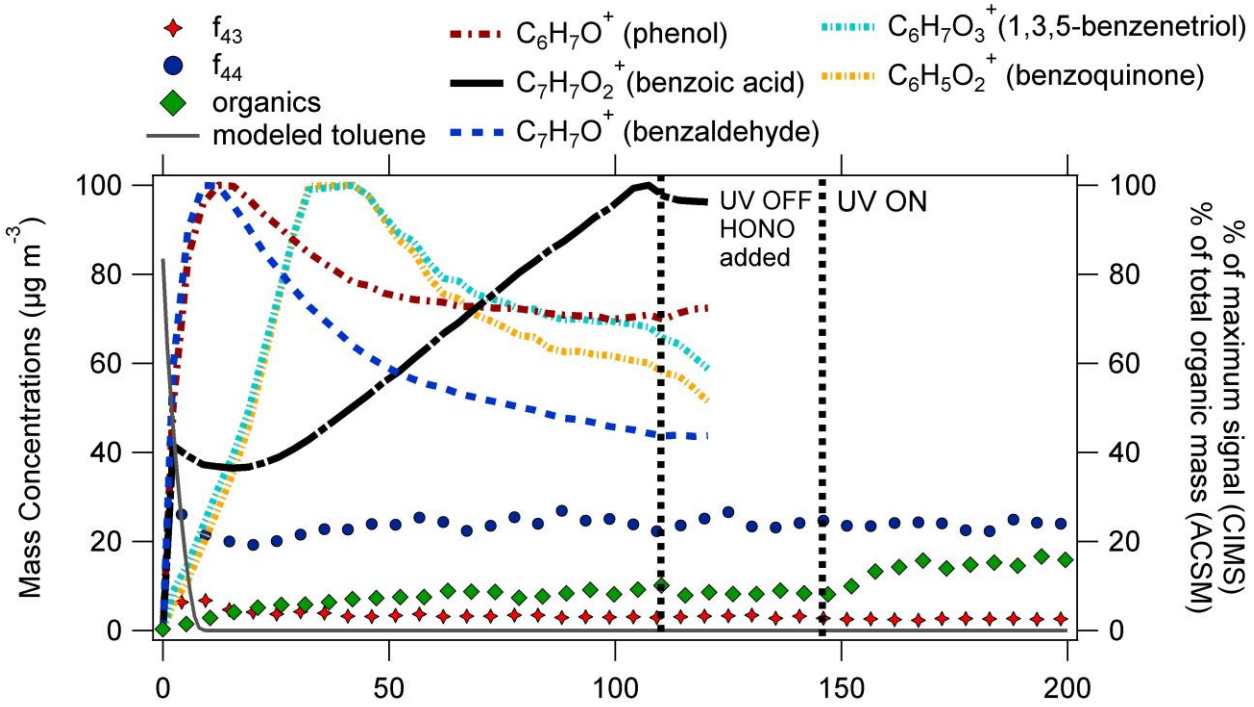

77

78 **Figure S8.** Time series of wall-loss corrected OA concentration and modeled toluene decay (left
79 vertical axis) and gas-phase products and f_{43}, f_{44} time series (right vertical axis) during
80 experiment 7 (Cl-High NO_x-OH). CIMS was offline after 120 minutes.

References for Supplementary Information

Cai, X., Ziemba, L.D., Griffin, R.J., 2008. Secondary aerosol formation from the oxidation of toluene by chlorine atoms, Atmos. Environ. 42, 7348-7359. doi:10.1016/j.atmosenv.2008.07.014

Carter, W.P.L., Cocker, D.R., Fitz, D.R., Malkina, I.L., Bumiller, K., Sauer, C.G., Pisano, J.T., Bufalino, C., Song, C., 2005. A new environmental chamber for evaluation of gas-phase chemical mechanisms and secondary aerosol formation. Atmos. Environ. 39, 7768–7788. doi:10.1016/j.atmosenv.2005.08.040

Cubison, M.J., Jimenez, J.L., 2015. Statistical precision of the intensities retrieved from constrained fitting of overlapping peaks in high-resolution mass spectra. Atmos. Meas. Tech. 8, 2333–2345. doi:10.5194/amt-8-2333-2015

Fantechi, G., Jensen, N.R., Saastad, O.L.E., Hjorth, J., Peeters, J., 1998. Reactions of Cl Atoms with Selected VOCs : Kinetics , Products and Mechanisms. J. Atmos. Chem. 31, 247–267. doi:10.1023/A:1006033910014

Hildebrandt Ruiz, L., Donahue, N.M., Pandis, S.N., 2009. High formation of secondary organic aerosol from the photo-oxidation of toluene. Atmos. Chem. Phys. 9, 2973–2986. doi:10.5194/acp-9-2973-2009

Huang, M., Liu, X., Hu, C., Guo, X., Gu, X., Zhao, W., Wang, Z., Fang, L., Zhang, W., 2014. Aerosol laser time-of-flight mass spectrometer for the on-line measurement of secondary organic aerosol in smog chamber. Meas. J. Int. Meas. Confed. 55, 394–401. doi:10.1016/j.measurement.2014.05.038

Huang, M., Zhang, W., Gu, X., Hu, C., Zhao, W., Wang, Z., Fang, L., 2012. Size distribution and chemical composition of secondary organic aerosol formed from Cl-initiated oxidation of toluene. J. Environ. Sci. 24, 860–864. doi:10.1016/S1001-0742(11)60840-1

Karlsson, R.S., Szente, J.J., Ball, J.C., Maricq, M.M., 2001. Homogeneous Aerosol Formation by the Chlorine Atom Initiated Oxidation of Toluene. J. Phys. Chem. A 105, 82–96. doi:10.1021/jp001831u

Wang, L., Arey, J., Atkinson, R., 2005. Reactions of chlorine atoms with a series of aromatic hydrocarbons. Environ. Sci. Technol. 39, 5302–5310. doi:10.1021/es0479437

Young, C.J., Washenfelder, R.A., Edwards, P.M., Parrish, D.D., Gilman, J.B., Kuster, W.C., Mielke, L.H., Osthoff, H.D., Tsai, C., Pikelnaya, O., Stutz, J., Veres, P.R., Roberts, J.M., Griffith, S., Dusanter, S., Stevens, P.S., Flynn, J., Grossberg, N., Lefer, B., Holloway, J.S., Peischl, J., Ryerson, T.B., Atlas, E.L., Blake, D.R., Brown, S.S., 2014. Chlorine as a primary radical: Evaluation of methods to understand its role in initiation of oxidative cycles. Atmos. Chem. Phys. 14, 3427–3440. doi:10.5194/acp-14-3427-2014